

## Short Communication

# Structure-based design of a bicyclic peptide antagonist of the vascular endothelial growth factor receptors

VICTOR GONCALVES,<sup>a,b</sup> BENOIT GAUTIER,<sup>a,b</sup> CHRISTIANE GARBAY,<sup>a,b</sup> MICHEL VIDAL<sup>a,b\*</sup>  
and NICOLAS INGUIMBERT<sup>a,b\*</sup>

<sup>a</sup> Université Paris Descartes, UFR biomédicale, Laboratoire de Pharmacochimie Moléculaire et Cellulaire, 45 rue des Saints Pères, Paris, F-75006, France

<sup>b</sup> INSERM U648, Paris, F-75006, France

Received 25 July 2007; Revised 26 September 2007; Accepted 28 September 2007

**Abstract:** Dysregulated angiogenesis is implicated in several pathologies, including cancer and age-related macular degeneration. A potential antiangiogenic strategy consists in developing VEGF receptor ligands capable of preventing VEGF binding and the subsequent activation of these receptors. Herein, we describe the structure-based design of a VEGF-mimicking peptide, VG3F. This 25-mer peptide was doubly cyclized, on-resin, by formation of both a disulfide bridge and an intramolecular amide bond to constrain it to adopt a bioactive conformation. Tested on *in vitro* assays, VG3F was able to prevent VEGF binding to VEGF receptor 1 and inhibit both VEGF-induced signal transduction and cell migration. Copyright © 2007 European Peptide Society and John Wiley & Sons, Ltd.

**Keywords:** angiogenesis; antagonist; Flt-1; peptide cyclization; vascular endothelial growth factor; VEGF receptor

## INTRODUCTION

Angiogenesis, the process of growing new blood vessels from an already established vasculature, is a fundamental biological mechanism, whose dysregulation results in several pathologies [1] such as cancer or age-related macular degeneration [2].

It is commonly admitted that among the various proangiogenic factors, the VEGF family, and especially the VEGF<sub>165</sub> isoform, is strongly involved in these pathologies [3]. VEGF<sub>165</sub> activity is triggered by its binding to three tyrosine kinase receptors (VEGFR1–3) located at the membrane of endothelial cells but also on several tumor cell lines (for review see Olson *et al.* [4])

Abbreviations: Acn, acetamidomethyl; AcOH, acetic acid; DCM, dichloromethane; DIPEA, *N,N'*-diisopropylethylamine; DMF, dimethylformamide; EA.hy926, hybrid cell line from human vascular endothelial cell line and human A549 lung carcinoma cell line; EGTA, ethylene glycol-bis(2-aminoethyl ether)-*N,N,N',N'*-tetraacetic acid; Flt, fms-like tyrosine kinase; FBS, fetal bovine serum; Fmoc, fluorenylmethoxycarbonyl; HBTU, O-benzotriazole-*N,N,N',N'*-tetramethyl-uronium-hexafluoro-phosphate; HNTG, hepes-NaCl-triton-glycerol; HOBt, N-hydroxybenzotriazole; HUVEC, human umbilical vein endothelial cell; KDR, kinase domain-containing receptor; MAPK, mitogen-activated protein kinase; NMP, 1-methyl-2-pyrrolidinone; Rink amide MBHA, 4-(2',4'-dimethoxyphenyl)-Fmoc-aminomethyl-phenoxycetamido-methyl benzhydryl amine; SDS, sodium dodecyl sulphate; TBS, tris-HCl buffer saline; TBST, tris-HCl buffer saline tween 20; TFA, trifluoroacetic acid; VEGF, vascular endothelial growth factor; VEGFR, vascular endothelial growth factor receptor; VEGFR1 d2, vascular endothelial growth factor receptor 1 domain 2.

\* Correspondence to: Michel Vidal, Nicolas Inguibert, Laboratoire de Pharmacochimie Moléculaire et Cellulaire, UFR biomédicale, 45 rue des Saints Pères, FR-75270 Paris Cedex 06, France;  
e-mail: nicolas.inguibert@univ-paris5.fr, michel.vidal@univ-paris5.fr

but only VEGFR-1 and 2 are implicated in angiogenesis while VEGFR-3 is responsible for lymphangiogenesis. Considering the central role of the VEGF<sub>165</sub>-VEGF receptors system, disrupting this interaction constitutes an attractive strategy for blocking pathological angiogenesis and therefore several strategies targeting either VEGF or its receptor have emerged [5]. One of the promising antiangiogenic approaches relies on the development of VEGFR ligands that are able to bind the receptor's extracellular domain and prevent their activation by the VEGF [6]. For the purpose of identifying such ligands, different strategies have emerged with the common objective of discovering VEGF-mimicking peptides, which would behave as receptor antagonists. Most of them reposed on the screening of peptide libraries obtained either by phage-display or by combinatorial peptide synthesis [7]. Structure-based approaches are rare despite the resolution of the three-dimensional structures of VEGF<sub>165</sub> alone [8] and of the complex VEGF<sub>8-109</sub>-VEGFR1 d2 [9] by X-ray diffraction. VEGF<sub>165</sub> is an antiparallel homodimeric protein and the link between the two monomers is ensured by two symmetrical disulfide bridges between Cys51 and Cys61 of  $\beta 1$  and  $\beta 1'$  strands. Furthermore, each VEGF monomer is characterized by an intrachain disulfide bonded knot motif at the core of the protein. Mutagenesis data [10,11] as well as structure-function studies allowed the identification of the VEGF amino acids involved in the recognition of its receptors (Figure 1). VEGFR1 d2 (green in Figure 1) is in contact with both subunits of the VEGF<sub>8-109</sub> and the contact surface is divided about 65%/35% between

each monomer. The segments of the first VEGF<sub>8-109</sub> monomer (blue in Figure 1) in contact with VEGFR1 d2 include residues from the *N*-terminal helix  $\alpha$ 1 (16–27), the loop connecting  $\beta$ 3 to  $\beta$ 4 (60–68) and the strand  $\beta$ 7 (103–106). The second monomer (red in Figure 1) interacts through the residues from strand  $\beta$ 2 (46–48) and from strands  $\beta$ 5 and  $\beta$ 6 together with the connecting turn (79–71). The structure of second monomer has been exploited by Zilberberg *et al.* [12] to design a 17-amino acid cyclic peptide, cyclo-VEGI [head-to-tail c(DFPQIMRIKPHQGQHIGE)] which mimicked the residues (79–93) and proved to be an antagonist of VEGF receptors with an IC<sub>50</sub> of 12  $\mu$ M measured on bovine aortic endothelial cells (BAE).

The aim of our work was to design a peptide named **VG3F** (for **VEGF 3** fragments), mimicking simultaneously the three fragments of VEGF involved in the interaction with VEGFR1 d2. **VG3F** is a peptide, cyclized by both a disulfide bridge and an amide bond established between two amino acid side-chains, the antagonist activity of which was assessed on endothelial cells models. Indeed this peptide is able to both inhibit MAPK activation and migration of cells in a wound healing assay induced by VEGF.

## RESULTS

### Peptide Design

The Figure 2 represents the three fragments of VEGF<sub>8-109</sub> in interaction with the surface of VEGFR1 d2 [9]. The  $\alpha$ -helix fragment (16–26 green in Figure 2) interacts with the receptor through five residues (Phe17, Met18, Tyr21, Gln22, Tyr25) situated at less than 4.5 Å from the receptor and located on a same face of the helix. These amino acids establish mainly hydrophobic interactions with the receptor and mutagenesis data corroborated their importance [11]. The  $\alpha$ -helix fragment is linked by a disulfide bridge established between Cys26 and Cys68 to the loop Cys60–Cys68 (red in Figure 2). This loop constitutes another major site for VEGFR1 binding as indicated by the Asp63Ala/Glu64Ala/Glu67Ala Ala-scan which

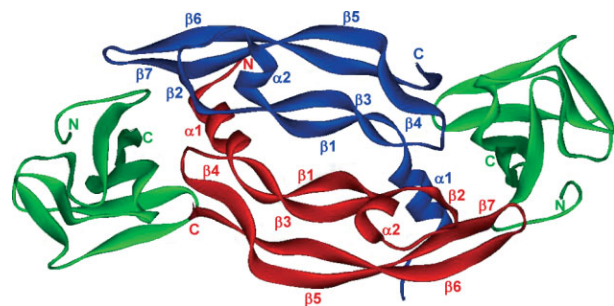


**Figure 1** X-ray structure of VEGF<sub>8-109</sub> in complex with VEGFR1 d2 (PDB code 1FLT).

induced a 30-fold decrease of affinity for VEGFR1. Moreover, the side chains of Arg224 from the receptor and Asp63 of VEGF are in ionic interaction. Lastly, the fragment Cys61–Cys68 is covalently linked in the VEGF to the  $\beta$ -strand (Cys102–Lys107) by the disulfide bridge Cys61–Cys104. Interestingly, these two fragments are also spatially closed with only 3.9 Å separating side-chain functions of Glu64 and Lys107. Furthermore, the lateral chains of Glu64 and Lys107 do not interact with the receptor.

Based on these data, we designed a single chain peptide that mimics simultaneously these three regions of VEGF. The Figure 3 depicts the structures of the VEGF fragments of interest and the sequence of the peptide **VG3F**. First, concerning the two disulfide bridges, we chose to conserve the one between Cys61 and Cys104 and to replace the other one linking Cys26 and Cys68 by a 6-aminohexanoic acid (Ahx) to connect the Tyr25 to the Glu67. Furthermore, to avoid oxidation issues we replaced the Cys60 by an isosteric Ser residue. Secondly, in order to maintain the spatial disposition of the three fragments we joined Ser60 to Glu103 by another Ahx linker and we introduced an additional conformational constraint by forming an

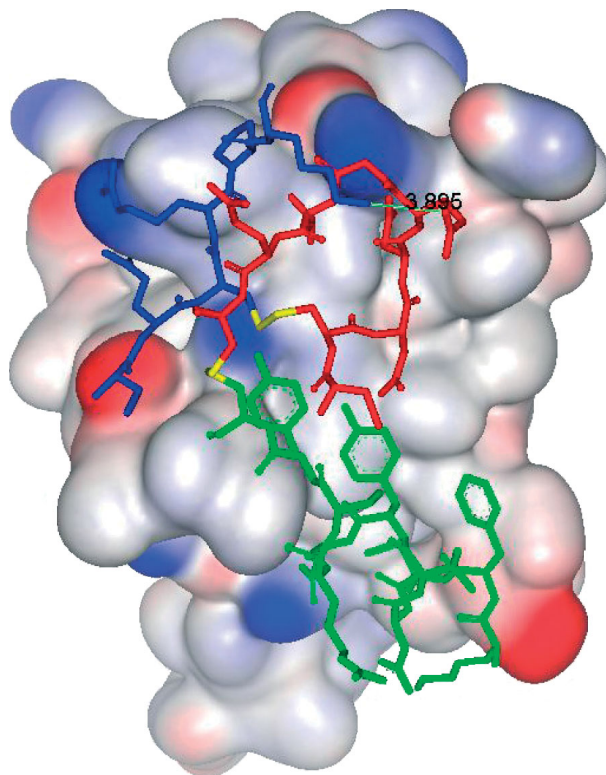


**Figure 2** X-ray structure of VEGF fragments 16–26 (green), 60–68 (red) and 102–107 (blue) in complex with VEGFR1 d2. The colored surface represents the electrostatic potential of VEGFR1 d2 surface. The disulfide bridges Cys26–Cys68 and Cys61–Cys104 are colored in yellow. The distance separating the side chain functions of Lys107 and Glu67 is indicated (3.9 Å).

amide bond between the lateral chains of Lys107 and Glu64 since these two chains are in a close spatial proximity of 3.9 Å. Lastly, considering that the peptide backbone was linked in the **VG3F** by Ahxs, the N → C orientation of the sequence Cys60–Glu67 needed to be inverted. As a result, we also had to invert the stereochemistry of the residues (59–67) by using D-amino acids. Thereby, the initial orientation of the side-chains, which ensure interactions with the receptor, was conserved.

### Synthesis of VG3F

The synthesis was performed by solid-phase peptide synthesis using Fmoc/tBu strategy (Scheme 1) [13]. This synthesis was supposed to perform two successive cyclizations of a 25-mer linear peptide. Such reactions, when performed in solution phase, usually lead to the formation of by-products resulting from the formation of interchain bonds rather than the expected intrachain bonds. To avoid this issue, we chose to perform the cyclizations on-resin (Resin substitution: 0.69 mmol/g). In this way, each peptide chain supported by the resin was relatively separated from the others, favoring intrachain resin-bound reaction by taking advantage of the pseudodilution phenomenon [14]. Cysteines were introduced as S-Acm protected amino acids, and the side chains of Glu64 and the Lys107 were protected respectively by the orthogonal protecting groups allyl and alloc. The elongation was carried out on a Rink amide MBHA resin on 0.25 mmol scale with *in situ*-activating reagents (HBTU, HOBt) in presence of DIPEA to generate HOBt esters. After each coupling a systematic acetylation of the residual N-terminus was performed with acetic anhydride. In

addition, we observed, in a previous attempt to perform this synthesis (data not shown), that couplings of Gly65, Glu67 and of the following Ahx were difficult. As a consequence, we realized a double-coupling for these residues. The elongation proceeded correctly except for Cys61 whose Fmoc deprotection peak was slightly weak. At the end of the synthesis, the N-terminal Fmoc protecting group was conserved and the peptidyl-resin was washed with NMP and DCM. Subsequently, the allyl and alloc protecting groups of Glu64 and Lys107 were cleaved on-resin by treatment with tetrakis(triphenylphosphine)palladium(0) for 3 h under argon atmosphere [15]. The coupling of the two lateral chains was performed with the previous coupling reagents overnight at room temperature. At this step of the synthesis, a sample of the resin was cleaved and deprotected and the crude mixture was analyzed by RP-HPLC giving a relatively clean profile considering the length of the peptide and the performed cyclization. Then, the peptide was subjected to an iodine oxidation [16] since such a treatment of the Acm protected cysteines results in simultaneous removal of the sulfhydryl protecting groups and disulfide bond formation between Cys61–Cys104. The peptidyl-resin was swollen in DMF and iodide in DMF was added dropwise under vigorous stirring. After 4 h reaction at room temperature, the resin was abundantly washed with DMF and DCM and a sample was taken for RP-HPLC analysis. This reaction of oxidation led to the formation of the expected peptide. Finally, the N-terminal Fmoc group was cleaved with 20% piperidine in DMF for 3 h and the peptide **VG3F** was cleaved from the resin and deprotected by treatment using TFA with thioanisole, triisopropylsilane and water as scavengers. The crude product was purified by semipreparative RP-HPLC on a C18 column giving pure **VG3F** (>94% by analytical HPLC) in 2.1% yield. The ESI-mass spectrum of **VG3F** was realized, confirming the sequence of the peptide.

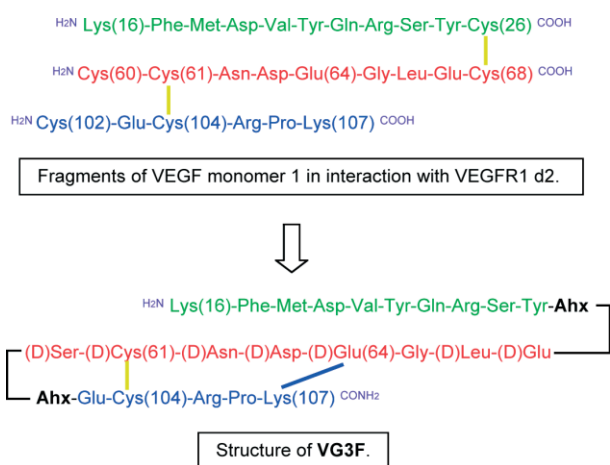
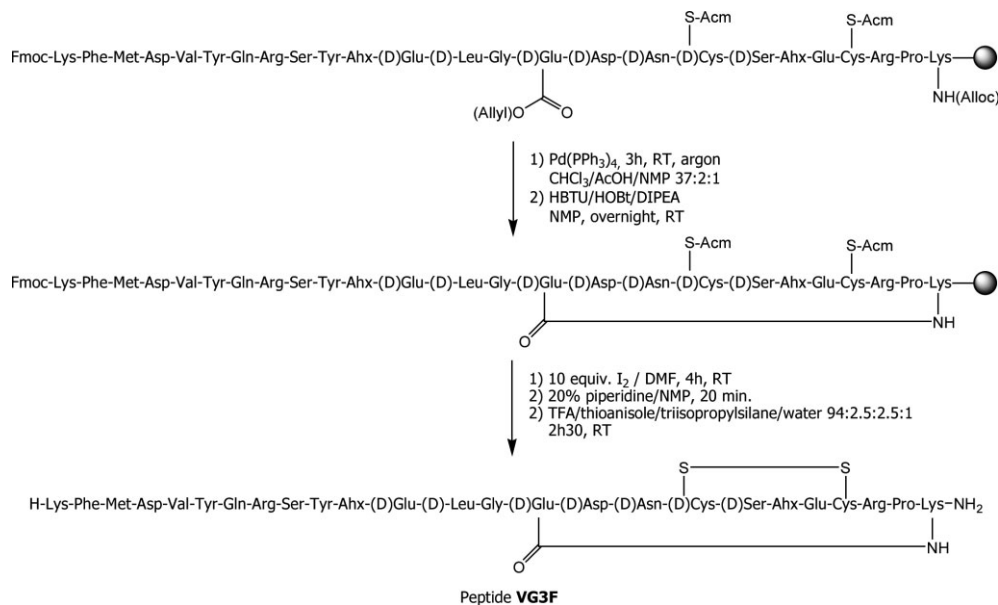


**Figure 3** Schematic representation of the VEGF fragments 16–26, 60–68 and 102–107 (A) and structure of the VEGF mimicking peptide **VG3F** (B). Yellow lines represent disulfide bridges. The blue line represents an amide bond established between Lys107 and Glu67 side-chain. Ahx: 6-aminohexanoic acid.

### Biological Evaluation

We undertook the biological evaluation of **VG3F** by determining its activity on a chemiluminescent assay relying on competition between the tested compound and biotinylated VEGF<sub>165</sub> for binding to recombinant human VEGFR1 [17]. The peptide appeared as a ligand of VEGFR1, able to prevent VEGF binding with an IC<sub>50</sub> of 52 μM while VEGFA exhibits an IC<sub>50</sub> of 0.800 nM in the same test. As a control, we also tested the peptide **SP5.2** (NGYEIEWYSWVTHGMY –NH<sub>2</sub>) identified by phage-display library screening by El-Mousawi *et al.* and described as a specific ligand of VEGFR1 [18]. This peptide exhibited an IC<sub>50</sub> of 28 μM in the competition assay. Despite the important gap between the two observed IC<sub>50</sub> for the natural and synthetic ligands, we investigated whether **VG3F** would display antagonist activities on endothelial cells. For this purpose, the



**Scheme 1** Synthesis of **VG3F**.

ability of the peptide to down-regulate VEGF-induced signal transduction was studied. One of the prominent effects triggered by VEGF binding to the VEGF receptors is the stimulation of cell proliferation through the activation of MAPK pathway [19]. Thereby, we examined by western blot whether the peptide was able to inhibit VEGF-induced phosphorylation of MAPK p42 and p44 (Figure 4). Tested at the dose of 100  $\mu\text{M}$ , **VG3F** inhibited significantly the phosphorylation of proteins validating this peptide as an antagonist of the VEGF receptors.

Finally, we searched to confirm this activity on a global cellular process, i.e. the VEGF-induced migration of endothelial cells. In this order, we tested **VG3F** on a 'wound healing assay' (Figure 5) [12]. Stimulation of starved cells by 520 pM of VEGF induced an increased cell migration compared to the negative control. Co-treatment of cells with 100  $\mu\text{M}$  of peptide and VEGF strongly inhibited their migration demonstrating the **VG3F** efficiency on biological processes involved in angiogenesis. The peptide **SP5.2** displayed the same profile of activity at 100  $\mu\text{M}$  than **VG3F** in these biological assays and, despite the high concentration

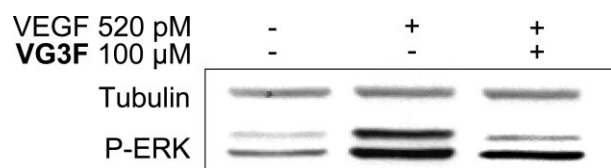


**Figure 4** Inhibition of VEGF-induced p44/p42 MAPK phosphorylation. Starved HUVEC, at confluence, were incubated with peptide **VG3F** at 100  $\mu\text{M}$  during 20 min, and then stimulated by VEGF 520 pM for 10 min. Western blot analysis was performed with antiphospho-p44/p42 MAPK and anti- $\gamma$ -tubulin as loading control. The figure shown is representative of two independent experiments.

of peptide employed in the experiments, no effect was observed on cell viability.

## CONCLUSION

In summary, the rational design of a VEGF mimicking peptide allowed us to synthesize a 25-mer peptide able to modulate VEGF-VEGFR1 interaction. The choice of performing the two cyclization reactions, on-resin, permitted to limit the formation of by-products and simplified the multistep synthesis. Considering the biological results observed for **VG3F**, this peptide could constitute a template for the design of shorter peptides that may conserve the same activity and may be used as vectors for specifically targeting endothelial cells.

## EXPERIMENTAL

### Generals

Rink amide MBHA resin was purchased from Novabiochem. HBTU, HOBt and DIPEA were from Applied Biosystems. Iodine and Pd(PPh<sub>3</sub>)<sub>4</sub> were from Fluka. All amino acids, from Novabiochem or Bachem, were N $^{\alpha}$ -terminal protected by Fmoc and their side chains were protected as follow: Arg(N-Pmc); Asn(N-Trt); Asp(O-All); Asp(O-tBu); Cys(S-Trt); Cys(S-Acm); Gln(N-Trt); Glu(O-All); Glu(O-tBu); His(N-Trt); Lys(N-Boc); Ser(O-tBu); Thr(O-tBu); Trp(N-Boc) and Tyr(O-tBu). Peptide synthesis solvents and acetonitrile for HPLC were of analytical grade and were acquired from commercial sources and used without further purification.

### Peptide Synthesis, Purification and Analysis

The peptide was synthesized by Merrifield stepwise solid-phase synthesis on an Applied Biosystems 433A automated

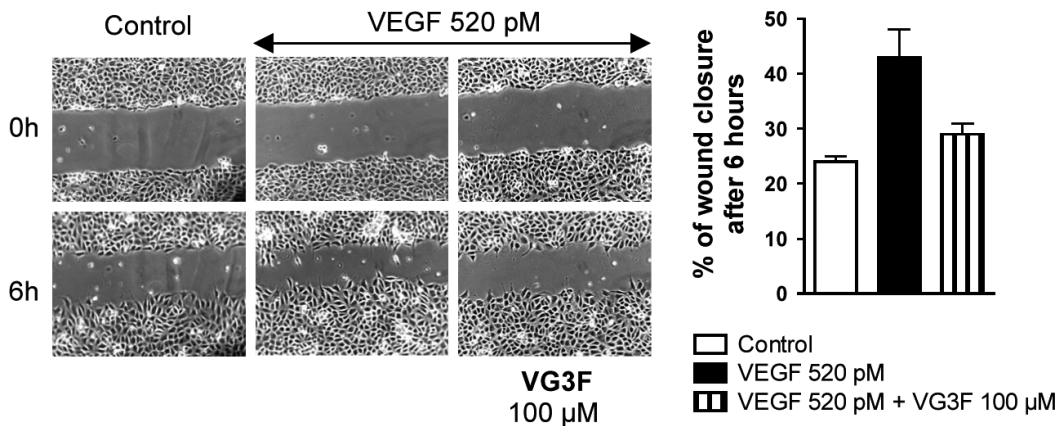


**Figure 5** Effects of the peptide on VEGF-induced cell migration in a wound healing assay. Confluent monolayers of starved EA.hy926 cells were wounded using a tip, and a set of photos was taken at this time. Then, cells were treated with 520 pM of VEGF alone or with **VG3F** at 100 μM and a second set of photos was taken 6 h later.

peptide synthesizer using standard scale (0.25 mmol) *FastMoc* chemistry. Coupling reactions were performed using Fmoc amino acids (4 equiv), activated with HBTU (4 equiv) and HOBt (4 equiv) in the presence of DIPEA (8 equiv), for 1 h. A capping was performed after each coupling by treatment with acetic anhydride capping solution (0.5 M acetic anhydride, 0.125 M DIEA, 0.015 M HOBt in NMP) for 5 min. Fmoc removal was realized by treating the resin with 20% piperidine in NMP for 15 min.

Once the elongation of the linear peptide was completed, the *O*-allyl and *N*-alloc protecting groups on Glu64 and Lys107 were removed by the following protocol: the resin was swollen in 26 ml of DCM/AcOH/NMP (37:2:1 v/v) and the suspension was bubbled with argon for 30 min. Then, 1.73 g of Pd(PPh<sub>3</sub>)<sub>4</sub> (3 equiv) were added and the solution was stirred for 3 h at room temperature under an argon atmosphere. The suspension was filtered and the resin was washed with a solution of 0.5% DIPEA in NMP (50 ml), a solution of diethyldithiocarbamate (0.5 g in 100 ml NMP), NMP (2 × 10 ml) and DCM (2 × 10 ml). Next, the peptidyl-resin was stirred overnight with a solution of coupling reagents (8 ml NMP + 0.25 ml 2 M DIPEA in NMP + 2.5 ml 100 mM HBTU in NMP) at room temperature and the resin was washed with NMP and DCM. Then, the resin was suspended in 170 ml of DMF and 70 ml of a solution of iodine in DMF (10 equiv.; 1.2 g) were added dropwise over 30 min. The solution was stirred vigorously for 4 h at room temperature. The solution was filtered and the resin was washed with 100 ml of DMF and DCM. Subsequently, the *N*-terminal Fmoc was cleaved by 20% piperidine in NMP for 20 min. Final peptide and samples were cleaved from resin with simultaneous removal of side-chain protecting groups by treatment with 15 ml TFA/water/ethanedithiol/triisopropylsilane (94/2.5/2.5/1 v/v) for 2 h 30 min at room temperature. The filtrate from the cleavage reaction was evaporated, precipitated in cold diethyl oxide, collected by centrifugation and lyophilized.

The crude peptide was purified by semipreparative RP-HPLC on a Nucleosil C18 column (Vydac, 5 μM, 10 × 250 mm) with a gradient program (solvent A is water with 0.1% TFA and solvent B is 70% acetonitrile aqueous solution with 0.09% TFA) at a flow rate of 2 ml/min with UV detection at 214 and 254 nm. Fractions were analyzed by RP-HPLC on a Nucleosil

C18 column (Vydac, 5 μM, 4.6 × 250 mm) at a flow rate of 1 ml/min and the pure fractions were collected and lyophilized to yield the final peptide as a white solid. The peptide identity was checked by electrospray mass spectrometry on a LCQ Advantage spectrometer (ThermoElectron, France). Yield after purification: 2.1% (**VG3F**, 4TFA); MS, *m/z* calculated for C<sub>130</sub>H<sub>200</sub>N<sub>36</sub>O<sub>40</sub>S<sub>3</sub>, 3003.39, found, 1002.3 [M + 3H]<sup>+</sup>/3 and 1502.5 [M + 2H]<sup>+</sup>/2; *t<sub>R</sub>* = 12.6 min (20–100% of solvent B in 40 min, purity >94%).

### Chemiluminescent Competition Assay on VEGFR1

The assay was performed as previously described by Goncalves *et al.* [38] Briefly, a fixed amount of biotinylated VEGF<sub>165</sub> (131 pM) was incubated with **VG3F** in presence of recombinant human VEGFR1 adsorbed on a 96-well microplate. The biotinylated VEGF<sub>165</sub> remaining after wash steps was detected by chemiluminescence—thanks to HRP-conjugated streptavidin.

### Cell Lines and Culture

HUVE cells were obtained as a gift from Dr Catherine Boisson-Vidal (U765 INSERM) and were cultured in 150-cm<sup>2</sup> plastic flasks, coated by a solution of 0.5% gelatin (BioChemika, Sigma), in M199 containing 20% FBS. Experiments were conducted on HUVEC that had gone through one to five passages. EA.hy 926 human cell line was obtained from Pr Cora-Jean S. Edgell (Pathology Department, University of North Carolina, Chapel Hill, USA). Cells were cultured in DMEM Glutamax-1 (Gibco Invitrogen), complemented with 10% FBS, 0.62% penicillin/streptomycin, and 2.5% HAT, from Gibco (Invitrogen). Cells were incubated at 37 °C in a humidified atmosphere of 5% CO<sub>2</sub> in air and medium was changed every 2–3 days.

### Western Blot Analysis

Experiments were realized in a 6-well plate coated with a solution of 0.5% gelatin. HUVEC, at confluence, were starved in 2% FBS-supplemented M199 overnight, followed by 5 h in 0% FBS-supplemented M199. HUVEC were

treated for 20 min with **VG3F** at 100  $\mu\text{M}$  in 0% FBS-supplemented M199, then stimulated by VEGF<sub>165</sub> at 520 pM for 10 min. Cells were washed three times with ice-cold PBS, and reaction was terminated by addition of 100  $\mu\text{l}$  of ice-cold lysis buffer HNTG : Hepes 50 mM, NaCl 150 mM, Glycerol 10%, Triton 100 1%, EGTA 1 mM, MgCl<sub>2</sub> 1 mM, Na<sub>3</sub>VO<sub>4</sub> 1 mM, NaF 1 mM and one protease inhibitor cocktail tablet (Complete, Roche). Equivalent amounts of proteins were resolved in 12% SDS-polyacrylamide gel and then transferred onto nitrocellulose membranes (Bio-Rad Laboratories). The transblotted membrane was incubated with antiphosphorylated p42/p44 MAPK antibody (Cell Signaling Technology, Beverly, MA, Etats-Unis) (1:1000) and with anti- $\gamma$ -Tubuline (Santa Cruz Biotechnology, Californie, Etats-Unis) (1:1000) in tris-buffered saline (TBS) containing 0.1% tween 20 (TBST) and 5% FBS at 4°C overnight. The immunoblots were visualized by enhanced chemiluminescence (Amersham Biosciences).

### Wound Healing Assay

EA.hy 926 cells were seeded in a 6-wells plate coated and were allowed to grow to confluence. Complete medium was replaced by medium containing 0% FBS, and incubation was continued overnight. A linear wound was drawn in the monolayer of cells. A set of digital photos was taken of each wound with a camera (Digital Sight, DS-L1, Nikon, Japon) at  $\times 100$  original magnification. The wells were washed with PBS, and medium containing 520 pM VEGF<sub>165</sub> alone or with the peptide **VG3F** at 100  $\mu\text{M}$ . After 6 h, a second set of photos was taken at the same place in the same conditions.

### Acknowledgements

Financial support for this work was provided by the Ligue nationale contre le cancer and by the University Paris Descartes Bonus-Qualité-Recherche grant. The authors thank Dr W.-Q. Liu for mass spectral data, Dr C. Boisson-Vidal and I. Galy-Fauroux for providing HUVE cells.

### REFERENCES

- Ferrara N, Gerber HP. The role of vascular endothelial growth factor in angiogenesis. *Acta Haematol.* 2001; **106**: 148–156.
- Carmeliet P, Jain RK. Angiogenesis in cancer and other diseases. *Nature* 2000; **407**: 249–257.
- Ferrara N, Gerber HP, LeCouter J. The biology of VEGF and its receptors. *Nat. Med.* 2003; **9**: 669–676.
- Olsson AK, Dimberg A, Kreuger J, Claesson-Welsh L. VEGF receptor signalling – in control of vascular function. *Nat. Rev. Mol. Cell Biol.* 2006; **7**: 359–371.
- Ferrara N. Vascular endothelial growth factor: basic science and clinical progress. *Endocr. Rev.* 2004; **25**: 581–611.
- Goncalves V, Gautier B, Lenoir C, Garbay C, Vidal M, Inguibert N. Peptides as antagonists of the VEGF receptors. *Pharmachem* 2006; 15–19.
- D'Andrea LD, Del Gatto A, Pedone C, Benedetti E. Peptide-based molecules in angiogenesis. *Chem. Biol. Drug Des.* 2006; **67**: 115–126.
- Muller YA, Christinger HW, Keyt BA, de Vos AM. The crystal structure of vascular endothelial growth factor (VEGF) refined to 1.93 Å resolution: multiple copy flexibility and receptor binding. *Structure* 1997; **5**: 1325–1338.
- Wiesmann C, Fuh G, Christinger HW, Eigenbrot C, Wells JA, de Vos AM. Crystal structure at 1.7 Å resolution of VEGF in complex with domain 2 of the Flt-1 receptor. *Cell* 1997; **91**: 695–704.
- Keyt BA, Nguyen HV, Berleau LT, Duarte CM, Park J, Chen H, Ferrara N. Identification of vascular endothelial growth factor determinants for binding KDR and FLT-1 receptors. Generation of receptor-selective VEGF variants by site-directed mutagenesis. *J. Biol. Chem.* 1996; **271**: 5638–5646.
- Muller YA, Li B, Christinger HW, Wells JA, Cunningham BC, de Vos AM. Vascular endothelial growth factor: crystal structure and functional mapping of the kinase domain receptor binding site. *Proc. Natl. Acad. Sci. U.S.A.* 1997; **94**: 7192–7197.
- Zilberberg L, Shinkaruk S, Lequin O, Rousseau B, Hagedorn M, Costa F, Caronzolo D, Balke M, Canron X, Convert O, Lain G, Gionnet K, Goncalves M, Bayle M, Bello L, Chassaing G, Deleris G, Bikfalvi A. Structure and inhibitory effects on angiogenesis and tumor development of a new vascular endothelial growth inhibitor. *J. Biol. Chem.* 2003; **278**: 35564–35573.
- Chang CD, Meienhofer J. Solid-phase peptide-synthesis using mild base cleavage of nalpha-fluorenylmethoxycarbonylamino acids, exemplified by a synthesis of dihydrosomatostatin. *Int. J. Pept. Protein Res.* 1978; **11**: 246–249.
- Mazur S, Jayalekshmy P. Chemistry of polymer-bound ortho-benzyne – frequency of encounter between substituents on cross-linked polystyrenes. *J. Am. Chem. Soc.* 1979; **101**: 677–683.
- Alcaro MC, Sabatino G, Uziel J, Chelli M, Ginanneschi M, Rovero P, Papini AM. On-resin head-to-tail cyclization of cyclotetrapeptides: optimization of crucial parameters. *J. Pept. Sci.* 2004; **10**: 218–228.
- Joseph CG, Wang XS, Scott JW, Bauzo RM, Xiang Z, Richards NG, Haskell-Luevano C. Stereochemical studies of the monocyclic agouti-related protein (103–122) Arg-Phe-Phe residues: conversion of a melanocortin-4 receptor antagonist into an agonist and results in the discovery of a potent and selective melanocortin-1 agonist. *J. Med. Chem.* 2004; **47**: 6702–6710.
- Goncalves V, Gautier B, Garbay C, Vidal M, Inguibert N. Development of a chemiluminescent screening assay for detection of vascular endothelial growth factor receptor 1 ligands. *Anal. Biochem.* 2007; **366**: 108–110.
- El-Mousawi M, Tchistiakova L, Yurchenko L, Pietrzynski G, Moreno M, Stanimirovic D, Ahmad D, Alakhov V. A vascular endothelial growth factor high affinity receptor 1-specific peptide with antiangiogenic activity identified using a phage display peptide library. *J. Biol. Chem.* 2003; **278**: 46681–46691.
- Cross MJ, Claesson-Welsh L. FGF and VEGF function in angiogenesis: signalling pathways, biological responses and therapeutic inhibition. *Trends Pharmacol. Sci.* 2001; **22**: 201–207.